C-NEXAFS Microanalysis and Scanning X-ray Microscopy of Microheterogeneities in a High-Volatile A Bituminous Coal

ARTICLE *in* ENERGY & FUELS · JANUARY 1995

Impact Factor: 2.79 · DOI: 10.1021/ef00049a012

6 AUTHORS, INCLUDING:

Harald Werner Ade
North Carolina State University
359 PUBLICATIONS **8,688** CITATIONS

SEE PROFILE

C-NEXAFS Microanalysis and Scanning X-ray Microscopy of Microheterogeneities in a High-Volatile A Bituminous Coal†

George D. Cody* and Robert E. Botto

Chemistry Division, Argonne National Laboratory, Argonne, Illinois 60439

Harald Ade

Department of Physics, North Carolina State University, Raleigh, North Carolina 27695

Sutinder Behal and Mark Disko

Exxon Research and Engineering Company, Annandale, New Jersey 08801

Susan Wirick

Department of Physics, SUNY at Stony Brook, New York 11794

Received June 6, 1994. Revised Manuscript Received September 16, 1994®

Carbon near-edge X-ray absorption microanalysis was applied to the study of the chemistry of macerals in ultrathin sections of a high-volatile A bituminous coal. High-resolution images were obtained by exploiting variations in the intensity of carbon-edge fine structure for contrast. The macerals vitrinite, cutinite, and sporinite were distinguishable based on the relative intensities of two prominent absorption bands. The lower energy band, at 285.5 eV, was assigned to the transition of the core (1s) electron to the valence π^* MO; the absorption intensity correlated with the concentration of aromatic carbon. The higher energy band, near 288 eV, was assigned to a transition of an electron from the core (1s) to a mixed Rydberg/valence (C–H*) state; the intensity of this band correlated with the concentration of aliphatic carbon. Inertinite's inner-shell spectrum was distinct from those of the other macerals by a relatively intense 1s–π^* absorption band, absorption due to transitions to higher energy π^* MO's associated with polynuclear aromatics, moderate absorption near 288 eV, and a shoulder at 289.5 eV which was assigned to oxygen containing functionality. At the highest energies, $E \sim 295$ eV, absorptions due to transitions to σ^* states were present in the carbon spectra of each maceral type.

Introduction

The microheterogeneous nature of coal has long been recognized as one of the foremost challenges in attempting to understand its molecular structure and its response to various process conditions. Some of this difficulty is alleviated through petrographic analysis. Reflected light microscopy has been the principal tool applied to the study of the textures, distributions, and associations of constituents in coals and other organic-rich sedimentary rocks. The identification and classification of coal's constituents as macerals has provided the systematics necessary for a thorough understanding of the physical and chemical properties of coal.

Differences in the optical properties of coal macerals, i.e., differences in $\% R_{\langle m \rangle}$, or more precisely, differences in the magnitudes of the real and imaginary parts of the dielectric constant at a given wavelength, relate to differences in maceral chemistry.[1,2] Bulk compositional and functional group information is not easily extracted from the optical properties of coal measured in the visible region of the electromagnetic spectrum. Notwithstanding these limitations, reflected light microscopy illuminates all of the textural complexity of coals through contrast on basis of reflectance properties alone.

Techniques for specific chemical analysis of coal's microheterogeneities fall into two categories: in situ characterization methods and analysis of physically separated maceral concentrates. In the latter case, isolation and concentration of macerals using density gradient centrifugation techniques allows for conventional chemical analysis using techniques such as FTIR, NMR, and GC/MS. Potential problems have been encountered; for example, it had been recognized that different chemistries and physical structures may be represented in particles with similar densities, i.e., a given density fraction may have more than one maceral type present.[3]

Conventional in situ analysis techniques include infrared microspectrophotometry,[4] microfluorospectral analysis,[5] and laser desorption and pyrolysis mass

† This work was performed under the auspices of the Office of Basic Energy Sciences, Division of Chemical Sciences, U.S. Department of Energy under contract No. W-31-109-ENG-38.

® Abstract published in *Advance ACS Abstracts,* November 1, 1994.

(1) van Krevelen, D. W. *Coal*; Elsevier: Amsterdam, 1961; 511pp.

(2) Cody, G. D.; Larsen, J. W.; Siskin, M.; Cody, G. D. *Energy Fuels* **1989,** *3,* 551.

(3) Dyrkacz, G.; Bloomquist, C. A. A. *Energy Fuels,* **1992,** *6,* 357.

0887-0624/95/2509-0075$09.00/0

Table 1. Characteristics of Pittsburgh No. 8 High-Volatile A Rank Bituminous Coal: APCS No. 4

% C[a]	83.0
% H	5.3
% O	9.0
% S	2.2
% ash	9.0
% vit.[b]	85
% lip.[c]	7
% inert.[d]	8

[a] On a weight percent basis. [b] Vitrinite. [c] Liptinite. [d] Inertinite.

spectrometry.[6] Each technique has been shown to be effective in elucidating chemical structural information regarding coal's microheterogeneities. At present, none of these techniques have a resolution better than 1 μm. Given a paucity of competing microanalytical techniques for characterizing organic compounds and considering the inevitable improvements in instrumentation and microfocusing technologies, continued contributions from these analytical techniques are assured.

A recent addition to the ensemble of in situ characterization methods techniques is scanning transmission X-ray microscopy (STXM), a powerful technique created through advances in X-ray microfocusing techniques and access to a high flux source of soft X-ray photons generated at synchrotron light sources. The capabilities of the STXM have been demonstrated with a variety of complex materials, including the analysis of chromosomes,[7] freeze-dried fibroblast cells,[8] polymer blends,[9] and human cartilage.[10] A preliminary application of the STXM to the analysis of the carbon chemistry of macerals demonstrated the utility of the technique as a probe of the chemical microheterogeneities in coal.[11] In the present paper, carbon NEXAFS microanalysis and imaging will be more extensively explored, applying STXM to the in situ analysis of a suite of macerals within a high-volatile bituminous coal.

Experimental Section

Samples. A high-volatile A bituminous coal from the Pittsburgh No. 8 seam was chosen for analysis. A summary of analytical data for this coal is presented in Table 1. The following caveat must be included; the chemical characteristics listed in Table 1 are obtained from column samples, while the experiments were performed on hand-picked specimen from individual blocks obtained from the same mines. An assessment as to how representative the data are is beyond the scope of the present work. In the future, with considerably more analysis, this important question can be addressed.

Sample Preparation. A crucial aspect of STXM and C-NEXAFS is the necessity of preparing extremely thin specimens. The relatively high molar absorption coefficient of carbon at these wavelengths, $\mu = 1 \times 10^4$ cm^2/g,[12] in addition to the high bulk density of carbon in coal requires that sample thicknesses be less than 800 nm. There are a variety of methods available to obtain specimens of this thicknesses. Three were selected: these are argon ion milling, ultramicrotoming, and surface grinding. Each technique was capable of achieving the required thicknesses; however, each was subject to its own special difficulties.

Sample thinning using argon ion milling involves the collision of an accelerated beam of Ar^+ ions into the surface of thin slab of material at a shallow angle. The entire process is performed under high vacuum (10^{-7} Torr) while the sample holder is cooled with liquid nitrogen. Although extremely thin regions were obtained, it was found that ion milling was generally unsatisfactory for producing large enough areas with uniform thickness for the STXM. Surface grinding produced reasonably large regions with acceptable thickness; however, scoring of the surface was prohibitively abundant in many cases.

Although a difficult technique to master, ultramicrotoming yielded the most favorable results. Thicknesses in the range of 100–200 nm were readily produced. There were still artifacts associated with the technique. For example, scoring marks paralleling the cutting direction of the diamond knife and chatter marks perpendicular to the cutting direction were often observed. Fortunately, these artifacts are highly uniform and, thus, were readily identifiable. A more insidious problem involved microfracturing of the coal parallel to the slicing direction of the knife. Only experience and extreme care can minimize these latter effects.

While the use of each thinning technique was explored, ultramicrotoming ultimately yielded the highest quality thin sections. Therefore, only data from the microtomed specimens have been presented below. It should be noted in general, however, that the quality of a given thinning technique may depend on the rank of coal under study.

Scanning Transmission X-ray Microscopy. The STXM is located at the National Synchrotron Light Source (NSLS) at Brookhaven National Laboratory (BNL). The microscope resides at the terminus of the X1A beam line extending from the soft X-ray undulator on the 2.5 GeV electron storage ring. The important elements of the instrument are a spherical monochromator, which is capable of a maximum 0.3 eV energy resolution, and the Fresnel, phase zone plate, which is used to focus the monochromatic X-ray beam. At its current capabilities the STXM has a resolution limit of 55 nm;[13] however, spatial resolution down to 10 nm may be possible in the future.[14] Transmission is measured using a gas-filled detector which counts X-ray photons passing through the sample. Details on the instrument's specifications have been reported elsewhere.[13,15]

In the present study the typical measurement protocol is as follows. After an interesting area was selected for high-resolution imaging, images were acquired at energies just below the carbon absorption edge (E < 282 eV), at several positions within the NEXAFS region of the edge ($E \sim 284$–300 eV) and on top of the edge (E > 310 eV). The rational for using this protocol is the following. Reductions in transmission at energies below the absorption edge are related to residual absorption, due to lower energy absorption edges, e.g., the chlorine L edge. Any spatial variations in intensity in this energy region should relate to variations in sample thickness or density. Similarly, at energies corresponding to the top of

(4) Brenner, D. In *Chemistry and Characterization of Coal Macerals*; Winans, Randall E, Crelling, John C., Eds.; ACS Symposium Series 252; American Chemical Society, Washington DC, 1984. Landais, P.; Rochdi, A. *Energy Fuels* **1990**, *4*, 290. Rochdi, A.; Landais, P. *Fuel* **1991**, *70*, 367.

(5) Lin, R.; Davis, A. *Org. Geochem.* **1988**, *10*, 473.

(6) Greenwood, P. F.; Zhang, E.; Vastola, F. J.; Hatcher, P. G. *Anal. Chem.* **1993**, *65*, 1937.

(7) Williams, S.; Zhang, X.; Jacobsen, C.; Kirz, J.; Lindaas, S.; Van't Hof, J.; Lam, S. S. *J. Microsc.* **1993**, *170*, 155.

(8) Zhang, X.; Williams, S.; Jacobsen, C.; Kirz, J.; Fu, J.; Wirick, S., manuscript in preparation.

(9) Ade, H.; Zhang, X.; Cameron, S.; Costello, J.; Kirz, J.; Williams, S. *Science* **1992**, *258*, 972.

(10) Buckley, C. J.; Burge, R. E.; Foster, S. Y.; Ali, C.; Scotchford, A.; Dunsmuir, J. H.; Ferguson, S. R.; Rivers, M. L. In *Soft X-ray Microscopy*; Jacobsen, C., Trebes, J., Eds.; Proceedings of SPIE; SPIE: Bellingham, WA, 1993.

(11) Botto, R. E.; Cody, G. D.; Kirz, J.; Ade, H.; Behal, S.; Disko, M. *Energy Fuels* **1994**, *8*, 152.

(12) *Center For X-Ray Optics, X-Ray Data Booklet*; Vaughan Douglas, Ed.; Lawrence Berkeley Laboratory, 1986.

(13) Jacobsen, C.; Williams, S.; Anderson, E.; Browne, M. T.; Buckley, C. J.; Kern, D.; Kirz, J.; Rivers, M.; Zhang X. *Opt. Commun.* **1991**, *86*, 351.

(14) Ade, H. *Synchrotron Radiation News* **1994**, *7*, 11.

(15) Kirz, J.; Ade, H.; Jacobsen, C.; C.-H. Ko, Lindass, S.; McNulty, I.; Sayre, D.; Williams, S.; Zhang, X. *Rev. Sci. Instrum.* **1992**, *63*, 557.

the carbon edge, variations in transmission relate to variations in the number of carbon atoms spatially. This number can vary due to changes in the carbon density or the sample thickness. In each case, spatial variations in X-ray transmission at the low and high energies can be compared with variations in intensity in the NEXAFS region. In this way, artifacts from sample preparation can be clearly differentiated from contrast based on chemically distinct microdomains.

A separate protocol is employed when obtaining carbon NEXAFS spectra. Each spectrum is obtained in triplicate and averaged. Background spectra were also obtained, again in triplicate and averaged. Energy calibration is as follows. A small amount of carbonaceous material present in the optical elements within the vacuum chamber contributes to the background absorption. A pronounced absorption band is observed in the background at 285.5 eV (when initially calibrated to a polystyrene standard). Each C-NEXAFS spectrum was calibrated to this band. Consequently, even given a slight error in the absolute energy, the relative energies of the inner-shell transitions are at least correct.

Results and Discussion

Introduction to NEXAFS. Prior to discussing the data, some introduction to NEXAFS is warranted. The utility of X-ray spectroscopy of polyatomic molecules is that one can obtain specific information on functional groups through the analysis of the fine structure preceding and superimposed on the absorption edge of a given atomic species.

The physics of NEXAFS is similar to valence shell electronic state spectroscopy with one important distinction; the initial state of the photoionized electron is in an atomic, not molecular, orbital. Herein lies the major advantage of inner shell over valence shell spectroscopy; the photoionized core hole is highly localized, and thus the initial orbital is more readily identified and, in principle, specific information on chemical bonding of an atom may be obtained. Absorption of X-rays occurs through the interaction of an X-ray photon with an electron in an atomic core resulting in the promotion of the inner-shell electron to a relatively low-lying unoccupied molecular orbital (LUMO). Molecules containing π orbitals generally have their lowest energy inner shell transition to the first unoccupied, or antibonding, π^* orbital. This transition is typically observed as a sharp and relatively intense absorption band with transitions typically in the range of 5−6 eV below the vacuum level. Even a relatively small molecule may exhibit numerous core to LUMO transitions. For example, in the case of benzene with six chemically equivalent carbons, transitions to the first and second π^* orbitals as well as higher energy σ^* orbitals occur, lending a fair degree of complexity to the carbon-edge fine structure.

In addition to transitions to π^* states, transitions to low-lying Rydberg states are possible and expected.[16,17] For atoms and simple polyatomic molecules, Rydberg transitions are observed as a series of absorption bands preceding the ionization threshold and decreasing in intensity and spacing with increased photon energy. The energy of the transitions are typically reported by their term values, TV, given by eq 1 as

$$\mathrm{TV} = R/(n - \delta)^2 \quad (1)$$

where TV is the energy difference between the specific Rydberg transition and the ionization potential of the excited atom, R is the Rydberg constant, n is the principal quantum number of the Rydberg orbital, and δ is the quantum defect.[16] There are a number of accessible Rydberg states, corresponding to different orbital angular quantum numbers, i.e., s, p, d, ..., etc., Rydberg orbitals. However, in the case of 1s inner-shell spectroscopy, electric dipole selection rules dictate that the transition from the 1s to an np Rydberg state is particularly intense.[18]

In alkanes, for example, a relatively intense absorption band is observed corresponding to the transition from carbon's 1s to a 3p Rydberg orbital. Such transitions are common in gas-phase inner-shell X-ray spectra,[19] as well as in electron energy loss spectra under conditions of small momentum transfer.[20] Transitions to Rydberg states are also observed in inner-shell X-ray spectra of condensed-phase aliphatic materials such as poly(ethylene)[17] and poly(propylene).[21] Recently, it has been recognized that in molecules with C−H bonds, significant mixing of the Rydberg orbital with a symetrically similar antibonding C−H* orbital occurs.[22] This mixing occurs at energies below the ionization potential and results in a relatively intense absorption band.[22]

As the incident photon energy is increased the ionization threshold is eventually exceeded, whereby the core electron may be completely removed from the influence of the core hole; i.e., the electron is promoted to the continuum. The position of the ionization potential is subject to a chemical shift which depends on the electronic environment surrounding the inner-shell electron. For example, IP's for carbon typically range from 290 to 296 eV; low values correspond to aliphatic and aromatic carbons and the higher values correspond to carboxyls,[23] the higher energies resulting from the higher electron affinity of the neighboring oxygen.

Above the ionization threshold, but still within the NEXAFS region, absorption bands due to transtions to various σ^* states are anticipated. Most 1s−σ^* transitions occur at energies greater than the ionization potential; therefore, the photoionized electron is only weakly associated with the core hole which leads to significant lifetime broadening of the absorption band.[17] In simple, diatomic molecules, the mean energy of the 1s−σ^* transition has been interpreted to result from resonant scattering of the photoionized electron wave between the excited core and neighboring atoms and has been shown to correlate with bond distance.[24] In polyatomic molecules, however, this relationship becomes more complex.

(16) Robin, M. B. *Higher Excited States of Polyatomic Molecules*; Academic Press: New York, 1974; Vol. I.
(17) Robin, M. B. *Higher Excited States of Polyatomic Molecules*; Academic Press: New York, 1985; Vol. III.
(18) Jaffé, H. H.; Orchin, M. *Theory and Application of Ultraviolet Spectroscopy*; John Wiley & Sons, Inc.: New York, 1962; 624pp.
(19) Sham, T. K.; Yang, B. X.; Kirz, J.; Tse, J. S. *Phys. Rev. A* **1989**, *40*, 652.
(20) Hitchcock, A. P.; Brion, C. E. *J. Electron Spectrosc. Relat. Phenom.* **1980**, *19*, 231.
(21) Ade, H.; Zhang, X.; Cameron, S.; Costello, C.; Kirz, J.; Williams, S. *Science* **1992**, *258*, 972.
(22) Stöhr, J. *NEXAFS Spectroscopy*; Springer-Verlag: New York, 1991.
(23) Jolly, W. L.; Bomben, K. D.; Eyermann, C. J. *At. Data. Nucl. Data. Tables* **1984**, *31*, 433.
(24) Sette, F.; Stöhr, J.; Hitchcock, A. P. *J. Chem. Phys.* **1984**, *81*, 4907.

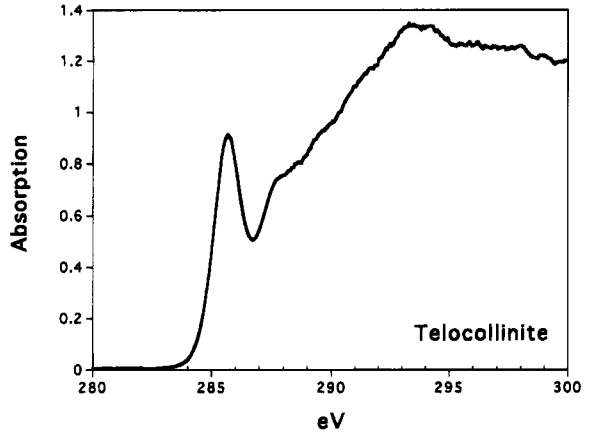

Figure 1. Carbon X-ray absorption spectrum of telocollinite (vitrinite).

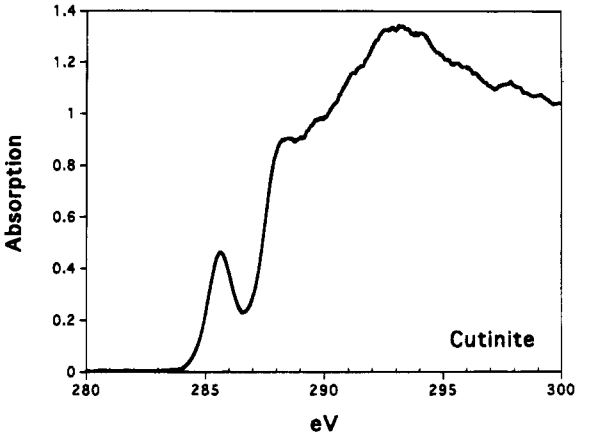

Figure 2. Carbon X-ray absorption spectrum of the maceral cutinite.

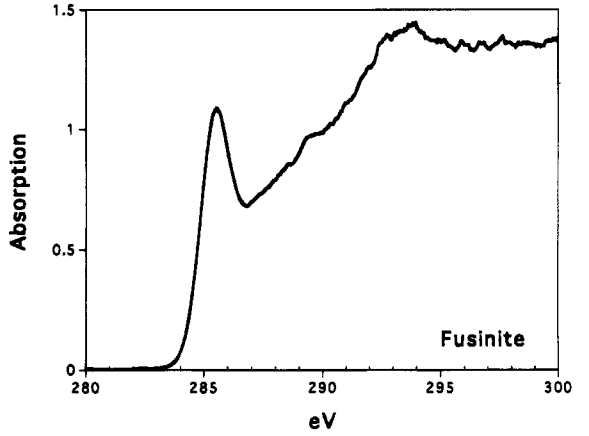

Figure 3. Carbon X-ray absorption spectrum of the maceral fusinite (inertinite).

In addition to the one-electron transitions that dominate the fine structure at the lower energies of the NEXAFS region, multielectron processes ("shake up" and "shake off" transitions) involving both inner-shell and valence electrons are possible at the higher energies.[16,17] However, these transitions occur well above the ionization threshold, in some cases considerably, e.g., up to 20 eV greater. Thus, they are not expected to contribute to the bulk of the NEXAFS spectra discussed in the present study.

Ultimately, in complex materials such as coal, the absorption-edge fine structure is obscured by a multiplicity of transitions to different states with similar energies. With the number of inequivalent carbons in coal presumably being fairly large, it would appear that deconvolution of C-NEXAFS is a difficult task. In the present work, however, it will be shown that some progress toward deconvolution can be made. Considering the potential of STXM to expose the compositional details of coal's microheterogeneities, the effort is certainly worthwhile.

STXM Analysis of Pittsburgh No. 8 High-Volatile A Bituminous Coal. Given the high spatial resolution of STXM, it remains the task of the operator to identify regions of interest and analyze them. Each sample was first explored using transmitted light microscopy; various macerals were located prior to STXM analysis. Fortunately, the macerals absorb weakly in the visible spectrum and the faint coloration allowed the various macerals to be identified even though the microtomed sections were extremely thin.

Figures 1, 2, and 3 show C-NEXAFS spectra from three different macerals classes. The spectrum presented in Figure 1 was obtained from a region of apparently homogeneous telocollinite (vitrinite). Among the different exinitic macerals identified, cutinite was relatively abundant; the carbon near-edge spectrum of this maceral is presented in Figure 2. Figure 3 presents the C-NEXAFS spectrum of a region that is presumed to be inertinite. This region exhibited relatively strong absorption in the visible spectrum evident using transmitted light microscopy. Morphologically, it appeared to be fusinite. As will be discussed below, the spectral features within each C-NEXAFS spectrum support these maceral assignments.

All of the C-NEXAFS spectra acquired for this coal exhibit a pronounced absorption band at ~285 eV (Table 2). The assignment of the transition is unambiguous;

Table 2. C-NEXAFS: Inner-Shell Transition Energies[a,b] and Assignments[c]

energy (eV)	vitrinite	cutinite	sporinite	inertinite
285.7	1s–π*(s)	1s–π*(w)	1s–π*(mw)	1s–π*(s)
288.1	Ryd/C–H*(m)	Ryd/C–H*(s)	Ryd/C–H*(s)	NR
289.5	NR	NR	NR	UA (m)
294.5	1s–σ*(m)	1s–σ*(s)	1s–σ*(m)	1s–σ*(w)

[a] Energy resolution of monochromator, 0.5 eV. [b] NR = not resolved, UA = assignment unknown. [c] Relative intensity given as (s) strong, (m) medium, (mw) medium weak, and (w) weak.

the absorption results from the photoinduced displacement of an electron from the core (1s) K shell orbital to lowest unoccupied π* molecular orbital. The presence of this transition is clearly related to the presence of aromatic carbon within the analyzed region.

Although, the intensity of the 1s–π* absorption correlates with the concentration of aromatic carbon, a measure of the absolute concentration based on peak intensity or area cannot be assessed. As is the case with all electric–dipole transition spectroscopies, absorption intensity is a function of the magnitude of the oscillator strength of the transition. Without an estimate of the oscillator strength it is impossible to be quantitative regarding the concentration of a given functional group responsible for an absorption. Given that the samples are quite uniform in thickness and assuming that the oscillator strength is the essentially same for aromatic carbon regardless of maceral type, it can be stated that the relative concentration of aromatic carbon is greatest

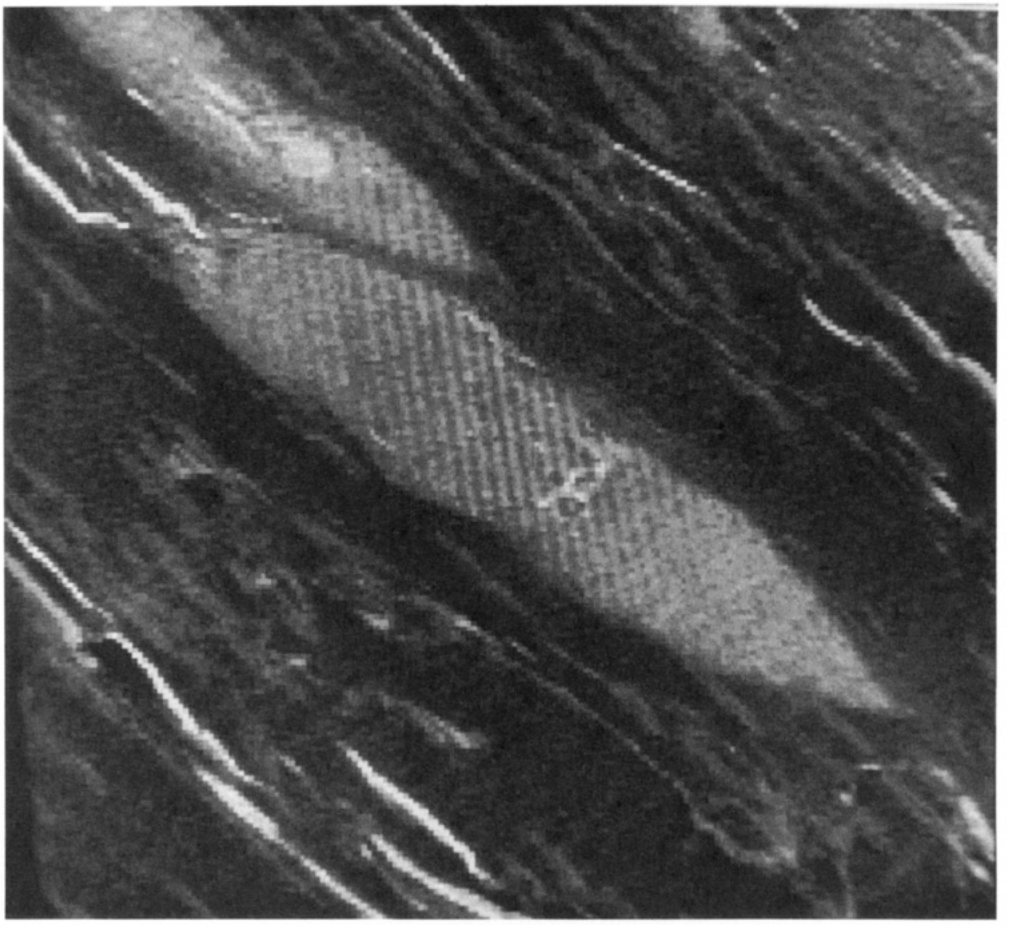

Figure 4. X-ray micrograph of Pittsburgh No. 8 high-volatile A rank coal. Monochromator set to 285.5 eV. Contrast is based on the concentration of aromatic carbon. Prominent elliptical bodies in upper left corner are identified as the maceral sporinite.

for the inertinite (Figure 3), least for the cutinite (Figure 2), and intermediate for the vitrinite (Figure 1).

While aromatic carbon bonded to hydrogen exhibits a $1s-\pi^*$ transition in the vicinity of 285 eV, aromatic carbon bonded to oxygen, as in the case of phenol, has its $1s-\pi^*$ transition shifted to higher energy, ~287 eV.[25] For a high-volatile bituminous coal, the concentration of phenol is anticipated to be low. However, in lower rank coals a substantial proportion of the aromatic carbon is bonded to oxygen, implying that their near-edge structure may be more complex than the spectra discussed in this paper.

Each C-NEXAFS spectrum exhibits a range of absorption fine structure in addition to the $1s-\pi^*$ transition. For example, clearly identified in Figures 1 and 2 are pronounced shoulders at ~288 eV. The shoulder is less well-defined in inertinite (Figure 2), principally because its intensity is masked by the relative strength of nearby absorption bands (Table 2). The occurrence of the 288 eV band is assigned to the transition from C(1s) to a mixed Rydberg/C−H* state of methyl and/or methylene carbon. Given that the ionization potential for protonated carbon is in the vicinity of 290.6 eV,[23] the term value (eq 1) for this transition is on the order of 2.5 eV. This indicates that the magnitude of the quantum defect term (eq 1) is on the order of 0.77 and suggests 3p character for the Rydberg state. This is in agreement with data from high-resolution gas-phase inner-shell spectra of a variety of pure methylated compounds.[16,20]

Absorption in this energy region may not be due entirely to the mixed Rydberg/C−H* transition. The presence of other functional groups may contribute to the absorption in the vicinity of 288 eV. For example, the $1s-\pi^*$ transition of carbonyl occurs at higher energies than aromatic carbon $1s-\pi^*$ transitions. In the case of formaldehyde, acetaldehyde, and acetone, strong absorptions have been observed at ~287 eV.[19,20] The $1s-\pi^*$ absorption of the carbonyl carbon in benzaldehyde occurs closer to 288 eV.[14,26] It has also been reported that C=O in formic acid exhibits a $1s-\pi^*$ transition at ~288 eV.[27]

C-NEXAFS spectra presented in Figures 1−3 clearly indicate that the intensity of the shoulder at approximately 288 eV is greatest for cutinite, intermediate for vitrinite, and the least for inertinite. This trend is consistent with the expected variation in chemical structure and composition of the macerals, implying that absorption at 288 eV is derived principally from the mixed Rydberg/C−H* transition of aliphatic carbon. As was the case with the $1s-\pi^*$ transition, it is not currently possible to be more quantitative in relating the intensity of the transition to the absolute concentration of aliphatic carbon, because the oscillator strength of the mixed Rydberg/C−H* transition in coal has not been determined.

The inner-shell spectrum of fusinite exhibits several features which are distinctly different than either vitrinite or cutinite. For example, several intense absorption bands appear between 286 and 288 eV. Absorption near 288 eV is presumably associated with a mixed Rydbergy/C−H* transition. The remaining absorption emanates from a least two additional sources. Aromatic carbon bonded to oxygen, i.e., in compounds

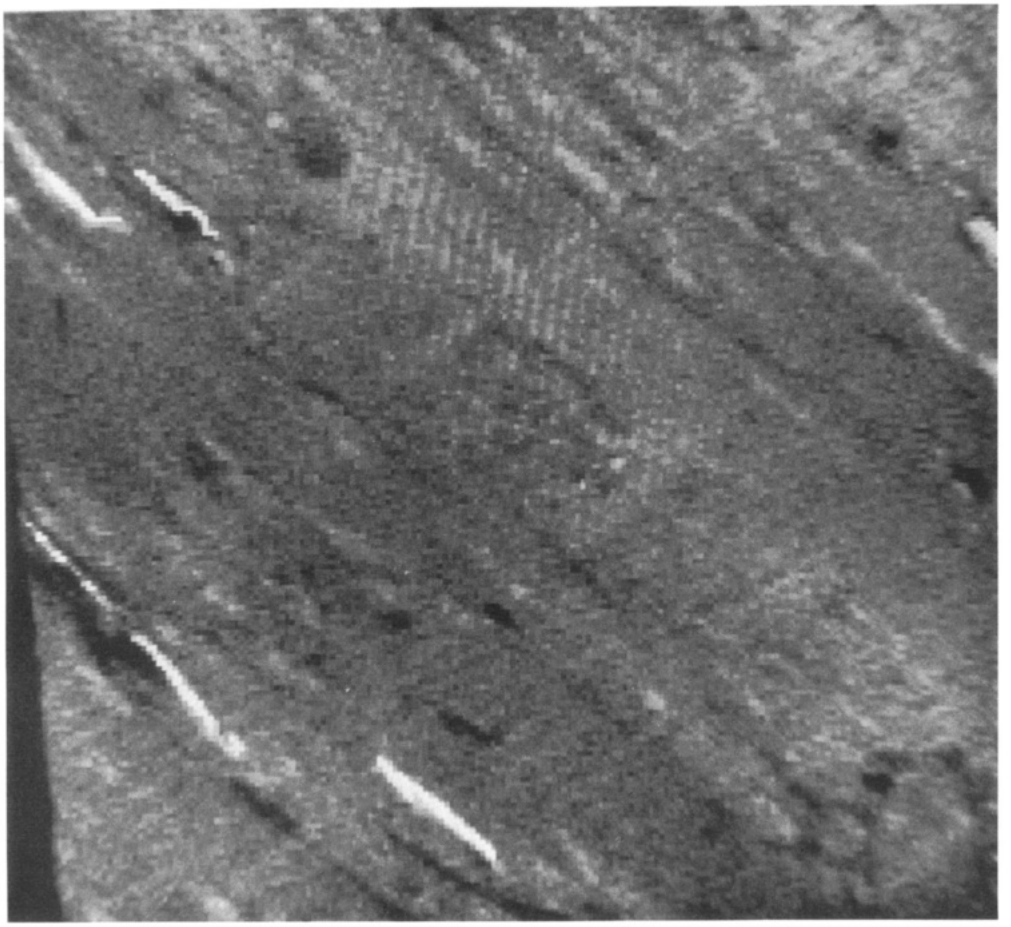

Figure 5. X-ray micrograph of Pittsburgh No. 8 high-volatile A rank coal. Monochromator is set to 288.1 eV. Contrast based on concentration of aliphatic carbon (see text). Note intracellular material within upper microspore, evident through contrast reversal when photon energy is shifted from 285.5 to 288.1 eV.

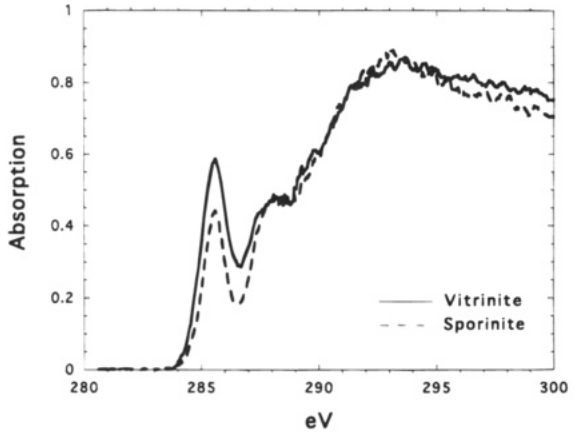

Figure 6. Carbon X-ray absorption spectrum of sporinite (dashed line); carbon X-ray absorption spectra of vitrinite adjacent to sporinite (solid line).

such as aryl ethers or hydroxylated aromatics, probably accounts for much of the intensity near 287 eV. Absorption nearer to 286 eV, however, may be assigned to transitions to higher energy π^* orbitals, as would be expected in polycondensed aromatic systems.

The pronounced shoulder at 289.5 eV is presumably related to carbonyl functionality. In an early application[28] of EELS to the study of carbon's inner-shell transitions related to molecular structure of nucleic acid bases revealed relatively strong absorption bands near 289 eV were assigned to C=O functionality in these compounds. The carbon inner-shell spectrum of benzoquinone exhibits a pronounced absorption band near 288.3 eV,[25] also related to the C=O functionality. However, the most salient feature in the C-NEXAFS spectrum of benzoquinone was a red shift of the lowest energy transition to near 283.7 eV.

C-NEXAFS analysis of benzaldehyde and analogous compounds exhibit an intense absorption band near 290 eV,[26] which results from the electronic transition to a relatively high energy π^* orbital. A relatively strong absorption peak, observed in NEXAFS spectra of both poly(ethylene terephthalate)[14,26] and poly(carbonate), has also been ascribed to the presence of this aromatic aldehydic functionality.[14]

Clearly, the differences manifested in fusinite's inner-shell carbon spectrum compared with the other macerals results from a higher degree of ring condensation, as well as greater quantity of oxygen-containing functional groups versus aliphatic structures. This chemistry is consistent with the origin of fusinite,[29] namely a fossil charcoal formed under the oxidizing conditions of a forest fire.

The feature observed at higher energies in each spectrum is a broad absorption band centered around

(25) Francis, J. T.; Hitchcock, A. P. *J. Phys. Chem.* **1992**, *96*, 6598.
(26) Hitchcock, A. P.; Urquart, S. G.; Rightor, E. G. *J. Phys. Chem.* **1992**, *96*, 8736.
(27) Ishii, I.; Hitchcock, A. P. *J. Chem. Phys.* **1987**, *87*, 830.
(28) Isaacson, M. *J. Chem. Phys.* **1972**, *56*, 1813.
(29) Dyrkacz, G. R.; Bloomquist, C. A. A.; Ruscic, L.; Horwitz, E. P. In *Chemistry and Characterization of Coal Macerals*; Winans, Randall E., Crelling, John C., Eds.; ACS Symposium Series 252; American Chemical Society: Washington, DC, 1984.

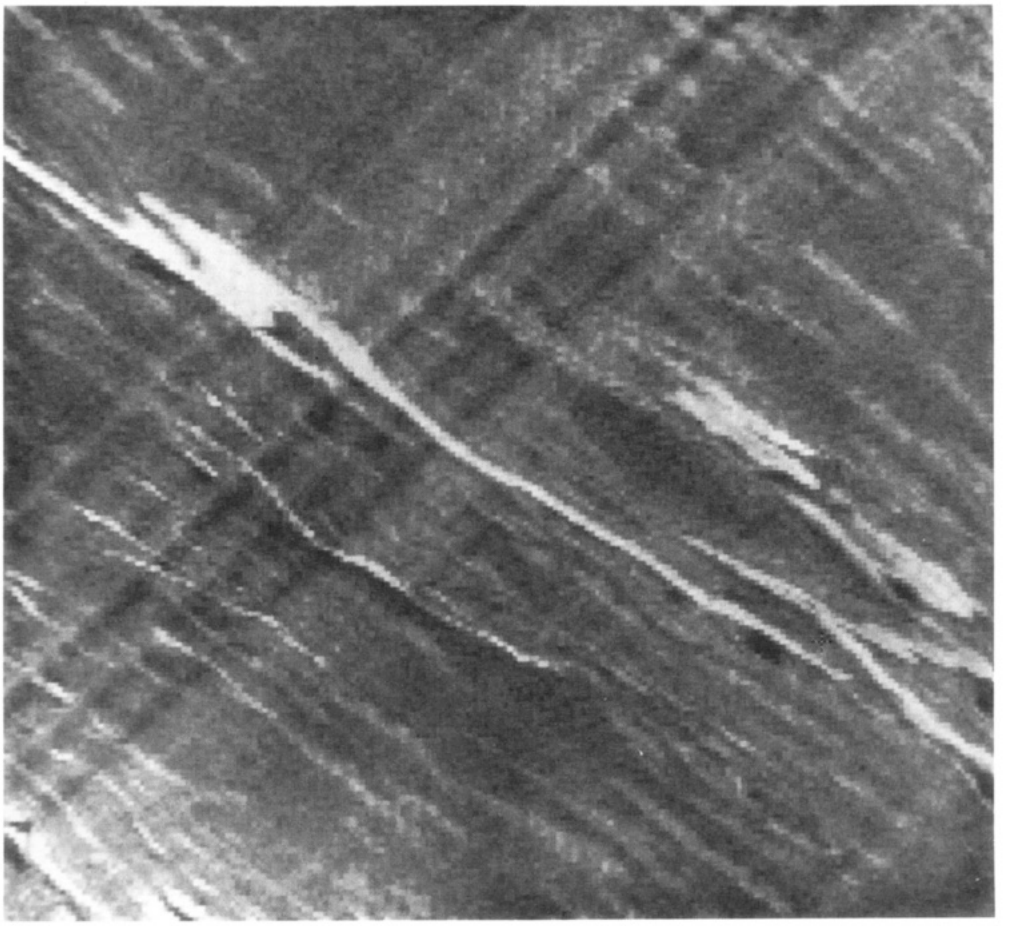

Figure 7. X-ray micrograph with monochromator fixed at 285.5 eV. A prominent ribbon of cutinite is nearly X-ray transparent indicating a low concentration of sp^2-hybridized carbon.

295 eV which is assigned to transitions from 1s to σ^* states. At present, this assignment is largely academic because both aromatic and aliphatic carbons contribute to the σ^* transitions and it is, currently, not possible to deconvolute their respective contributions. However, it is noteworthy that this absorption band is relatively narrow in the cutinite spectra, while considerably broader in the case of vitrinite, sporinite, and inertinite. Whether the broadening is due to differences in the lifetimes of the excited states in the different maceral groups or to another phenomenon cannot be determined at this time; however, the differences observed are most certainly related to differences in molecular structure of each maceral.

Superimposed on the bound-state absorption structure is absorption associated with ionization of an electron into the continuum. Not much can be said specifically about the exact shape of this absorption plateau. Considering the types of carbons expected in this coal a range of ionization potentials starting at approximately 290 eV ranging up to 294 eV is expected.[30] Such a distribution would suggest a steplike rise to the absorption plateau.

STXM Imaging of Macerals. The advantage of the X-ray microscope is that it exploits variations in absorption-edge fine structure for the purpose of obtaining images with chemically specific information. A demonstration of this capability is presented in Figures 4 and 5. Considering the inner-shell spectra (see Figures 1−3), it is evident that the optimum choice for probing spatial variations in carbon chemistry is to compare images obtained at 285.5 and 288.1 eV, corresponding to the absorption energies of sp^2- and sp^3-hybridized carbons, respectively.

Imaging with the monochromator tuned to 285.5 eV provides a high level of contrast, clearly evident in Figure 4. Dominating the field of view is a pair of elliptical structures identified as the maceral sporinite, i.e., an exinitic maceral derived from structurally preserved microspores.[31] Reflected light microscopy of this sample supports this identification. Figures 4 and 5 are transmission images; darker areas are regions of higher absorption which correspond to higher concentrations of either sp^2- and sp^3-hybridized carbon depending the photon energy. Shifting the monochromator to an energy of 288.1 eV results in the microspores being no longer discernible. Analysis of the spectra in Figure 6 demonstrates why this is so. Although the differences in the concentration of aromatic carbon are clearly indicated through differences in the intensity of the 1s−π^* transition, the concentration of sp^3-hybridized carbon within the microspores and surrounding vitrinite appears comparable, evident in strengths of their respective absorption at 288.1 eV.

A subtle, but important, feature appears in the center of the upper microspore (Figure 4); this is the highly

(30) Wagner, C. D.; Riggs, W. M.; Davis, L. E.; Moulder, J. E.; Muilenberg, G. E. *Handbook of X-ray Photoelectron Spectroscopy*; Perkin-Elmer: USA, 1979.

(31) Stach E.; Mackowsky, M.-Th.; Teichmuller, M.; Taylor, G. H.; Chandra, D.; Teichmuller, R. *Stach's Textbook of Coal Petrology, 3rd Edition*; Gebruder Borntraeger: Stuttgart, Germany, 1982.

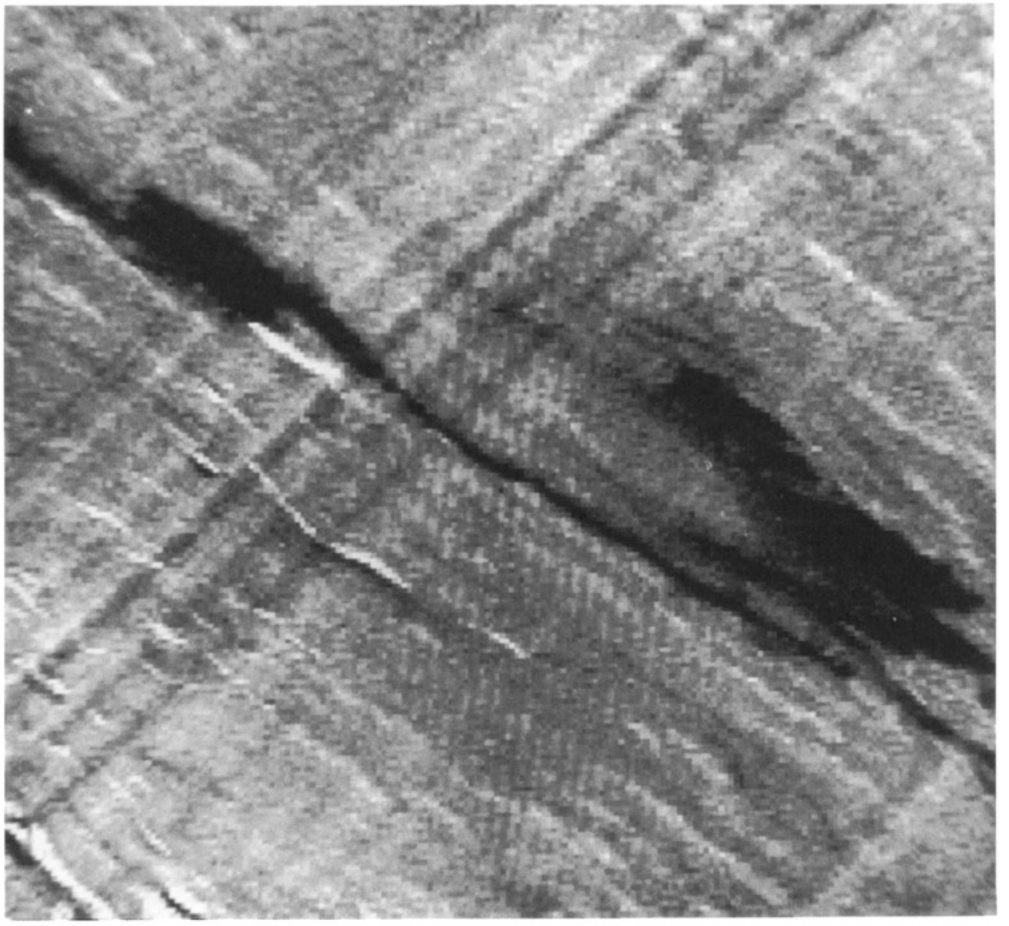

Figure 8. X-ray micrograph with monochromator fixed at 288.1 eV. Cutinite is strongly absorbing at this energy consistent with a high content of sp^3-hybridized carbon.

X-ray transparent region, approximately 2 μm in diameter. Proximal to this region are two very thin features that are also highly transmitting. When the monochomator is tuned to a photon energy of 288.1 eV (Figure 5) both regions now strongly absorb. Thus, the core of the fossil microspore undergoes a contrast reversal, whereas the spore's outer rim or "exine" does not. Whether the core material is an original constituent of the microspore or mobile aliphatic-rich material which had later migrated into void space within the core of the microspore cannot be discerned. However, the potential for preserved intracellular material in ancient microspores is exciting and warrants further investigation.

Other exinite macerals such as cutinite, exhibit a striking reversal in contrast relative to adjacent vitrinite, when images are acquired at 285.5 and 288.1 eV. Inspection of the spectra in Figures 1 and 2 reveals the reversal in relative absorption intensity of the primary spectral features in cutinite and vitrinite. Figures 7 and 8 demonstrate the utility of this phenomenon with a field of view containing cutinite, which is clearly evident as a very thin ribbon transecting the image. While highly transmitting at 285.5 eV, cutinite becomes nearly opaque at 288.1 eV (Figure 8), demonstrating that cutinite is highly aliphatic relative to the surrounding vitrinite.

Comparing the two exinitic macerals, sporinite, and cutinite, one observes (see Figures 2 and 6) significant differences in their respective chemistries. Cutinite is clearly more aliphatic than sporinite. Such chemical variability within the fundamental maceral classes is not surprising and has been suggested previously.[32]

Table 3. Ratio of the Intensity of the 1s$-\pi^*$ to Ryd/C$-$H* Transitions: APCS No. 4 Macerals

maceral	$(I_{\pi^*}/I_R)_{ave}$	no. spectra	std dev
vitrinite	1.17	17	0.07
cutinite	0.49	5	0.07
sporinite	0.91	5	0.09
fusinite	1.39	1	NA

Compositional Variability of Macerals in Pittsburgh No. 8. In this initial investigation of C-NEXAFS microanalysis of coals, numerous cutinite, sporinite, and vitrinite spectra have been obtained. It is compelling to assess the range in their compositions from the C-NEXAFS data, acknowledging that these data are preliminary and may not be wholly representative of the Pittsburgh No. 8 seam.

As a qualitative measure of aromatic carbon content it is proposed that the intensities of the 1s$-\pi^*$ and mixed Rydberg/C$-$H* transitions be ratioed. A number of vitrinite, cutinite, and sporinite spectra were acquired, while only one spectrum of inertinite was obtained. Table 3 summarizes the data for the four macerals. Each maceral type is clearly distinct from the others and the ratioes parallel that which is expected considering what is known regarding maceral chemistry. While the results of this analysis are not terribly surprising, they demonstrate the utility of

(32) Winans, R. E.; Crelling, J. C. *Chemistry and Characterization of Coal Macerals*; ACS Symposium Series 252; American Chemical Society: Washington DC, 1984.

STXM and the crucial importance of obtaining selective C-NEXAFS spectra of the constituents. Without the selectivity that C-NEXAFS affords, analysis of the whole coal will be a composite with spectral contributions spanning a wide range of absorption intensities. It is clear that such an analysis would be of limited value when applied toward understanding the molecular structure of coals.

Conclusions

The results from the application of the STXM as a probe of the chemistry of macerals within coals is extremely promising. In light of this promise, the pace of X-ray spectroscopic research is increasing. Expansion of the sample set to lower and higher rank coals will enable us to probe the geochemical evolution of coal macerals during diagenesis and catagenesis. Exploration of sapropelic coals with extremely complex microtextures has already begun. In addition to carbon, the energy regions including oxygen's 1s and calcium and chlorine's 2s transitions are being explored. Future publications will report on these findings.

Acknowledgment. This work was performed at the National Synchrotron Light Source (NSLS) which is supported by the Department of Energy. G.D.C. gratefully acknowledges the Chemistry Division of Argonne National Laboratory for support granted through the award of the Enrico Fermi Scholarship. G.D.C. and R.E.B. acknowledge support from the Office of Basic Energy Sciences, the Department of Energy, under contract No. W-31-109-ENG-38. SW and the STXM Facility are supported by the Department of Energy, DOE/OHER, under contract No. 89ER60858. The authors extend their gratitude to Janos Kirz, Chris Jacobsen, and Xiadong Zhang of the Department of Physics, SUNY Stony Brook, for their assistance and to Russel Cook and Nestor Zaluzec of the Material Science Division, Argonne National Laboratory, for their advice and assistance.

EF9401031